12-1-2013

Can Inhibitor-Resistant Substitutions in The Mycobacterium Tuberculosis β-Lactamase BlaC Lead to Clavulanate Resistance?: A Biochemical Rationale for The Use of β-Lactam–β-Lactamase Inhibitor Combinations

Sebastian G. Kurz
University Hospitals Case Medical Center

Kerstin A. Wolff
University Hospitals Case Medical Center

Saugata Hazra
Albert Einstein College of Medicine

Christopher R. Bethel
Louis Stokes Cleveland Veterans Affairs Medical Center

Andrea M. Hujer
Case Western Reserve University

See next page for additional authors

Authors
Sebastian G. Kurz, Kerstin A. Wolff, Saugata Hazra, Christopher R. Bethel, Andrea M. Hujer, Kerri M. Smith, Yan Xu, Lee W. Tremblay, John S. Blanchard, Liem Nguyen, and Robert A. Bonomo

Can Inhibitor-Resistant Substitutions in the *Mycobacterium tuberculosis* β-Lactamase BlaC Lead to Clavulanate Resistance?: a Biochemical Rationale for the Use of β-Lactam–β-Lactamase Inhibitor Combinations

Sebastian G. Kurz, Kerstin A. Wolff, Saugata Hazra, Christopher R. Bethel, Andrea M. Hujer, Kerri M. Smith, Yan Xu, Lee W. Tremblay, John S. Blanchard, Liem Nguyen, Robert A. Bonomo

The current emergence of multidrug-resistant (MDR) and extensively drug-resistant (XDR) tuberculosis calls for novel treatment strategies. Recently, BlaC, the principal β-lactamase of *Mycobacterium tuberculosis*, was recognized as a potential therapeutic target. The combination of meropenem and clavulanic acid, which inhibits BlaC, was found to be effective against even extensively drug-resistant *M. tuberculosis* strains when tested *in vitro*. Yet there is significant concern that drug resistance against this combination will also emerge. To investigate the potential of BlaC to evolve variants resistant to clavulanic acid, we introduced substitutions at important amino acid residues of *M. tuberculosis* BlaC (R220, A244, S130, and T237). Whereas the substitutions clearly led to *in vitro* clavulanic acid resistance in enzymatic assays but at the expense of catalytic activity, transformation of variant BlaCs into an *M. tuberculosis* H37Rv background revealed that impaired inhibition of BlaC did not affect inhibition of growth in the presence of ampicillin and clavulanate. From these data we propose that resistance to β-lactam–β-lactamase inhibitor combinations will likely not arise from structural alteration of BlaC, therefore establishing confidence that this therapeutic modality can be part of a successful treatment regimen against *M. tuberculosis*.

Despite the introduction of effective combination chemotherapy more than 50 years ago, tuberculosis (TB) remains a major cause of suffering and mortality worldwide (1). The necessity of prolonged treatment regimens, in conjunction with the notorious propensity of *Mycobacterium tuberculosis* to develop drug resistance, sets the stage for the development of multidrug-resistant (MDR) and extensively drug-resistant (XDR) strains. Major factors contributing to the current rise in MDR and XDR TB are the HIV pandemic and failing public health programs (2, 3).

Recently, combinations of β-lactams and β-lactamase inhibitors have been recognized as potential therapeutic options for treatment of MDR and XDR TB (4). The *M. tuberculosis* β-lactamase, BlaC, belongs to Ambler class A (5, 6), members of which are generally susceptible to the β-lactamase inhibitors that are currently used in the clinic: tazobactam, sulbactam, and clavulanate (7). Indeed, *in vitro* studies indicate that clavulanate significantly reduces the MICs of *M. tuberculosis* to most β-lactam antibiotics (4, 8–10). In particular, the early bactericidal activity of amoxicillin/clavulanate was comparable to that of antituberculosis drugs other than isoniazid (11). Recently, the combination of clavulanic acid with meropenem was found to be highly effective against XDR isolates of *M. tuberculosis* (12). Moreover, the use of meropenem and clavulanic acid as part of a salvage regimen was recently reported to show promising results (13). Unfortunately, meropenem must be delivered intravenously, thereby limiting its widespread use as prolonged therapy. The need exists to find the "right partner" to accompany clavulanic acid.

The atomic structures of BlaC, either as an apo enzyme or in complex with substrates and inhibitors, have shed light on the important structure-function relationships that define the efficacy of β-lactam–β-lactamase inhibitor combinations (10, 12, 14, 15). A comparative analysis of BlaC with other class A structures revealed some notable differences. In TEM and SHV β-lactamases, the most studied class A enzymes, the carboxylate group of the substrate forms hydrogen bonds to the R244 and to the sequence K234-T235-G236, which is referred to as the carboxylate-binding region (KTG motif) (16). Interestingly, R244 is replaced by alanine while A220 is changed to arginine in the BlaC sequence. As a result of this difference, investigators have hypothesized that R220 plays the same role in substrate binding and recognition as R244 (17–21). Downstream of the KTG motif, BlaC possesses a threonine at the 237 position (usually an alanine in other class A enzymes [7]), which was also found to participate in carboxylate binding (22–30). (Fig. 1) This region plays an important dual role in the recognition and activation of clavulanate and other so-called mechanism-based inhibitors. These bind to the active site similarly to substrates and then undergo a secondary ring opening, which leads to formation of reactive intermediates, resulting in prolonged inhibition (31–33). In other class A enzymes, several amino acids that confer relative resistance to mechanism-based inhibitors have been identified. Generally, substitutions at these

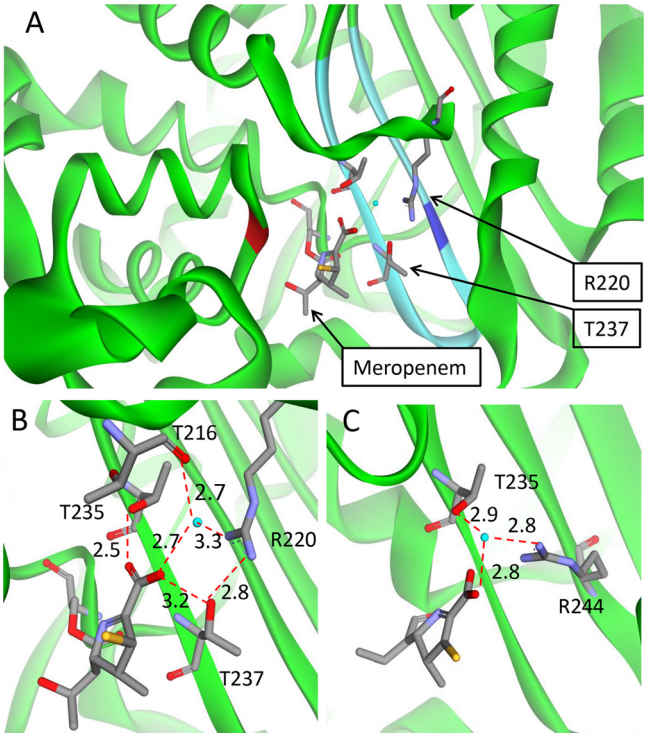

FIG 1 Enzyme structures of BlaC wild type—comparison with SHV-1. (A) BlaC with meropenem bound as an acyl-enzyme. The residues subjected to mutagenesis are highlighted. The A244 position is in dark blue and the S130 position is in red on the ribbon (PDB entry 3DWZ). (B and C) Meropenem interaction with the carboxylate binding site of BlaC (PDB entry 3DWZ) (B) and in comparison with SHV-1 (C). Note the different positions of the guanidinium group in BlaC (R220) versus SHV-1 (R244).

sites also lead to an overall reduction in beta-lactam affinity. To illustrate, substitutions at position R244 or N276 of SHV-1 lead to different levels of resistance to ampicillin, in both cases well above the clinically relevant breakpoints. However, different levels of resistance to ampicillin-clavulanate are seen with each of these substitutions which may translate into different inhibitor-resistant phenotypes (34).

With the above notions in mind, we sought to determine if substitutions in important amino acids impair the ability of clavulanic acid to inhibit BlaC and, as a result, jeopardize the use of future β-lactamase–inhibitor combinations against *M. tuberculosis*. Based on observations with other class A enzymes, we focused on Ambler positions 220, 244, and 237 of the carboxylate-binding region, as well as S130 (Fig. 1A). To this end, we assessed the effect on enzymatic activity, as well as the susceptibility of the variant *M. tuberculosis* strains to the ampicillin-clavulanate combination.

MATERIALS AND METHODS

Protein expression and mass spectrometry. A pET28-based plasmid carrying a truncated sequence of *blaC* (Δ_{1-39}*blaC*) (35) was used as the template for site-directed mutagenesis of Ambler positions R220, A244, S130, and T237 as previously described (36), using mutagenic primers. Primers used in this procedure are listed in Table 1. After the mutations were confirmed by sequencing, the plasmids expressing 6His-tagged BlaC mutant proteins were electroporated into *Escherichia coli* BL21/DE3 cells, and protein expression was induced with 1 mM isopropyl β-D-1-thiogalactopyranoside (IPTG) at an optical density at 600 nm (OD_{600}) of 0.8. After incubation for 18 h at 16°C, cells were harvested and lysed using a QIAexpress nickel-nitrilotriacetic acid (Ni-NTA) fast-start kit, followed by nickel column purification of the His-tagged protein according to the manufacturer's protocol (Qiagen Inc., Valencia, CA). To remove the His tag, the eluted protein was incubated with thrombin (Novagen, Madison, WI) overnight at 4°C (1.6 units per mg protein). The cleaved protein was separated from the 6His tag peptides by size exclusion chromatography using a HiLoad 16/60 Superdex 75 column (GE Healthcare Life Science, Uppsala, Sweden).

Mass spectrometry. The sizes of all generated proteins were determined using electrospray ionization (ESI) mass spectrometry (MS). Spectra were generated on an Applied Biosystems (Foster City, CA) QStar Elite quadrupole time-of-flight mass spectrometer equipped with a TurboIon spray source. Protein samples were desalted using a C_{18} ZipTip (Millipore, Billerica, MA) following the manufacturer's protocol. Eluted proteins were diluted with 50% acetonitrile and 0.2% formic acid. The samples were infused at a rate of 0.5 μl/min, and data were collected for 2 min. Spectra were deconvoluted using the Applied Biosystems Analyst program (Framingham, MA).

Kinetic analysis. Steady-state kinetics were performed on an Agilent 8453 diode array spectrophotometer (Agilent, Palo Alto, CA) in sodium phosphate buffer (50 mM, pH 7.2) and a 1-cm-path-length cuvette. V_{max} and K_m were determined from initial steady-state velocities for nitrocefin (NCF) ($\Delta\varepsilon_{482}$ = 17,400 M^{-1} cm^{-1}) and ampicillin ($\Delta\varepsilon_{235}$ = −900 M^{-1} cm^{-1}). The kinetic parameters were obtained using iterative nonlinear least-squares fit of the data to the Henri-Michaelis equation using Origin 8.0 (OriginLab, Northampton, MA) according to the following equation: $v = V_{max}[S]/(K_m + [S])$.

A plateau of steady-state velocities was only observed at very high substrate concentrations, which impaired the ability to determine K_m and k_{cat} in a precise manner. However, the ratio of k_{cat}/K_m remained stable during serial experiments and hence is a more accurate reflection of enzyme properties.

Given the high K_m for NCF even with the wild-type enzyme, the desire to choose substrate concentrations well above the K_m was balanced against the negative impact of high NCF concentrations on viscosity of the reactant solution and the precision of spectroscopic measurements. Therefore, NCF was used at 100 μM for wild-type enzyme (about double the K_m of NCF; results were corrected for K_m of NCF) and 200 μM for mutant enzymes.

We determined the K_i for the inhibitors by measuring initial steady-state velocities in the presence of a constant concentration of enzyme with increasing concentrations of inhibitor against the indicator substrate NCF (100 μM for wild-type enzyme and 200 μM for mutant enzymes). Assuming a competitive mode of inhibition, initial velocity (v_0) measurements immediately after mixing yield a K_i which closely approximates K_m, as repre-

TABLE 1 Primers used

Primer	Sequence (5′–3′)
BlaC-R220A-F1	CACCGGAGCCAAGGCCATCCGAGCGGGCTTTC
BlaC-R220A-R1	GAAAGCCCGCTCGGATGGCCTTGGCTCCGGTG
BlaC-R220S-F1	CCGGAGCCAAGAGCATCCGAGCGGGCTTTC
BlaC-R220S-R1	GAAAGCCCGCTCGGATGCTCTTGGCTCCGG
BlaC-S130G-F1	GCGATACGCTATGGCGACGGCACCGC
BlaC-S130G-R1	GCGGTGCCGTCGCCATAGCGTATCGC
BlaC-T237A-F1	ACAAGACCGGGGCCGGTGACTACGGA
BlaC-T237A-R1	TCCGTAGTCACCGGCCCCGGTCTTGT
BlaC-T237S-F1	GACAAGACCGGGAGCGGTGACTACGGA
BlaC-T237S-R1	TCCGTAGTCACCGCTCCCGGTCTTGTC
BlaC-A244R-F1	GGTGACTACGGACGACGCAACGACATCGCGGTC
BlaC-A244R-R1	GACCGCGATGTCGTTGCGTCGTCCGTAGTCACC
BlaC-NdeI	CATATGCGCAACAGAGGATTCGGTCG
BlaC-SalI	GTCGACTGATATCGATCGCCACTAC

sented by the following equation: $v_0 = (V_{max}[S])/(K_m(1 + K_i) + [S])$, where [S] represents substrate concentration.

IC_{50}, defined as the inhibitor concentration resulting in a reduction of NCF (μM) hydrolysis by 50%, was determined by measurements of initial velocities after 5 min preincubation of enzyme with inhibitor.

K_i values were corrected for nitrocefin affinity according to the following equation: $K_i(corr) = K_i(obs)/(1 + [NCF]/K_{mNCF})$.

Strain construction. The full-length *blaC* gene was PCR amplified from *M. tuberculosis* genomic DNA using primers BlaC-NdeI and BlaC-SalI (Table 1). The DNA fragment was then cloned into the integrative vector pMV361 (37) using NdeI and SalI restriction enzymes. Site-directed mutagenesis was performed as described above, and the mutations were confirmed by sequencing.

Competent cells of the parental *M. tuberculosis* strain H37Rv and its derived Δ*blaC1* mutant (PM638) (38) were prepared as described previously (39). Plasmids expressing wild-type and variant BlaC enzymes were transformed into competent cells by electroporation (39). Transformants were selected on 7H10 (Difco) agar medium supplemented with 0.05% Tween 80, oleic acid-albumin-dextrose-catalase (OADC) (BD), and kanamycin (50 μg/ml) at 37°C.

Antibiotic susceptibility testing. Antibiotic susceptibility testing of *M. tuberculosis* strains for ampicillin and clavulanate was performed using microtiter plate assays with 14 days of incubation, as previously described (40).

Immunoblotting. A polyclonal rabbit antibody was raised against the truncated BlaC protein (Josman, LCC, Napa, CA) and was purified using protein G column purification (GE Healthcare Life Science). *M. tuberculosis* strains were grown in roller bottles containing 100 ml 7H9 (Difco) medium supplemented with 0.05% Tween 80 and OADC (BD) at 37°C over 14 days. The bacteria were harvested by centrifugation and resuspended in Tris-buffered saline (TBS) containing proteinase inhibitor cocktail (Roche). Cells were pelleted and frozen at −80°C. After thawing, the cells were resuspended in 2 ml phosphate-buffered saline (PBS) containing proteinase inhibitors. Cells were disrupted by sonication on ice. Unbroken cells and cell debris were removed by centrifugation (4,000 rpm, 15 min) at 4°C.

Proteins in cell lysates were separated on SDS-PAGE gels and transferred to a polyvinylidene difluoride membrane (Invitrogen). The membrane was blocked using 5% bovine serum albumin (BSA) in TBS (20 mM Tris-HCl [pH 7.4], with 150 mM NaCl) overnight. After being washed with TBS, the membrane was incubated with the purified anti-BlaC antibody (0.2 μg/ml) in TBS containing 5% BSA for 2 h. The membrane was washed in TBS containing 0.05% Tween 20 (TBS-T) and incubated with protein G-horseradish peroxidase conjugate (Bio-Rad) at a 1:20,000 dilution for 1 h. After being washed with TBS-T, the blot was developed using an enhanced chemiluminescence (ECL) developing kit (GE Healthcare Life Sciences) according to the manufacturer's instructions. Purified truncated BlaC was used as a control. Sensitivity was assessed using serial dilutions of the purified BlaC protein.

Crystallization. The hanging drop vapor diffusion method was used for crystallization of BlaC-R220A. The composition of the well consists of 0.1 M HEPES (pH 7.5) and 2 M $NH_4H_2PO_4$, which makes the final pH of the well solution 4.1. Protein at a concentration of 12 mg/ml was mixed 1:1 with the well solution and incubated at 10°C. The mutant was initially seeded with the native enzyme crystals, and then after iterative crystal growths, the pure mutant crystals were obtained. Iterative microseeding resulted in efficient crystal growth as well as improved morphology, producing diffraction-quality crystals of the mutant enzyme. Glycerol (20%) was added to the solution as a cryoprotectant.

Data collection and refinement. Data were collected at the Brookhaven National Laboratory on line X29. The data were processed using HKL2000 (41). A previous structure of the apo *M. tuberculosis* β-lactamase (10) (PDB entry 2GDN) was used to phase the data, using the CCP4 software suite (42). Multiple rounds of structural refinement and model building were performed in Refmac5, Phenix (43–45), and Coot (46).

TABLE 2 AMU calculated and measured by mass spectrometry

Mutation(s)	AMU (Da)[a]	
	Calculated	Measured (±3)
None (wild type)	28,784	28,784
R220A	28,699	28,699
R220S	28,715	28,716
R220A, A244R	28,784	28,785
S130G	28,754	28,754
T237A	28,754	28,755
T237S	28,770	28,771

[a] AMU, atomic mass unit. ±3 indicates the error range in Da.

Structure figures were generated using PyMOL (47). For data collection statistics for the structures as well as the final refinement statistics, see Table 6.

Homology modeling and minimization. The crystal structures of the BlaC R220A mutant and wild-type BlaC (PDB entry 2GDN) were used as templates for homology modeling of R220S, R220A-A244R (template, R220A mutant), and S130G (template, PDB entry 2GDN), respectively. The molecular visualization program SWISS PDB Viewer was used to manipulate the position of amino acid residues. The predicted model was also checked for psi and phi torsion angles using the PDBsum Ramachandran plot (48). The initially found model was further improved by the steepest-descent energy minimization method using the GROMACS software package (49, 50). After 5,000 steps of steepest-descent minimization had been performed, the molecular dynamics simulation for 300 ps was carried out to examine the quality of the model structures and check its stability. Finally, the stereochemical quality of the model was checked by the PROCHECK method. PyMOL (47) and XMGrace (51) were used to analyze and to prepare structural diagrams.

Molecular docking. Molecular docking for this study was carried out by using the program AutoDock Vina 1.1.2 (69). Vina utilizes its global search algorithm to find the best binding pose after a thorough docking calculation. The three-dimensional (3D) structure of meropenem was downloaded from RCSB protein data bank from cocrystal structure (PDB entry 3DWZ). The 2D structure of clavulanate was made by using ChemDraw Ultra 8.0 and transformed to a 3D structure using Chem3D Ultra 8.0 (70). After that the two ligands were parameterized using the PRODRG2 server (71). The AutoDock tool (ADT) (72) had been extensively used to prepare all the structures and setup the docking protocol. The BlaC R220A was used as a static receptor. All the polar hydrogens were assigned, nonpolar hydrogens were merged, and PDBQT files were created by adding Gasteiger charges to the receptor as well as for the ligands. The AutoTors utility of ADT was used to define all possible torsions of the rotatable bonds of ligands. A grid map around the receptor active site was defined with the dimensions of 20 × 20 × 20 points, a grid center of −4.0 × −1.0 × 90.0, and spacing of 1.0 Å between the grid points. All the docking calculations were run to produce 10 docking poses for each ligand. The docked poses with the highest binding affinities were considered for further analysis.

Protein data accession number. Atomic coordinates and experimental structure factors have been deposited in the Protein Data Bank (PDB ID 4JLF).

RESULTS

Production of variant BlaC proteins. Primers for site-directed mutagenesis were designed to introduce single amino acid substitutions at Ambler positions 220 (R → A and R → S), 130 (S → G), and 237 (T → A and T → S) using a plasmid containing wild-type $\Delta_{1\text{-}39}$*blaC* (truncated) as the template (Table 1). The mutated plasmids were transformed into *E. coli* DH10B by electroporation. Plasmid-containing colonies were selected on LB agar containing

TABLE 3 Catalytic activities of wild-type and variant enzymes

Mutation(s)	Nitrocefin			Ampicillin		
	K_m (μM)	k_{cat} (s^{-1})	k_{cat}/K_m ($\mu M^{-1}\ s^{-1}$)	K_m (μM)	k_{cat} (s^{-1})	k_{cat}/K_m ($\mu M^{-1}\ s^{-1}$)
None (wild type)	56 ± 4	75 ± 2	1.34 ± 0.1	44 ± 2	16.8 ± 0.2	0.4
R220A	587 ± 103	5 ± 1	0.01	2,100 ± 350	18 ± 2	0.01
R220S	2,230 ± 830	31 ± 10	0.01	511 ± 334	8 ± 3	0.02
R220A, A244R	394 ± 37	35 ± 2	0.1	1,600 ± 1,124	64 ± 33	0.04
S130G	641 ± 87	13 ± 1	0.02	2,847 ± 1,311	25 ± 9	0.01
T237A	630 ± 100	17 ± 2	0.03	700 ± 83	42 ± 3	0.06
T237S	130 ± 4	74 ± 1	0.57	64 ± 11	6 ± 0.3	0.1

Values are least square fits for the Henri-Michaelis equation (see "Kinetic analysis" in Materials and Methods) ± standard errors (errors of ±10% have been omitted for clarity). See Materials and Methods for a discussion of methodological limitations.

kanamycin (20 μg/ml). The mutant *bla* genes were confirmed by sequencing of both strands of the derived plasmids. A second mutation (A244R) was later introduced into the plasmid containing $blaC_{R220A}$. Plasmids expressing mutant *bla* genes were then transformed to *E. coli* BL21/DE3 cells by electroporation and transformants selected on kanamycin agar. The variant enzymes were expressed and purified. All proteins were purified to homogeneity (>95%). SDS-PAGE analysis revealed single bands of similar sizes for all variant enzymes. Electrospray ionization-mass spectrometry (ESI-MS) was used to measure atomic mass and confirm identity (Table 2).

Kinetic characterization of variant enzymes. Table 3 summarizes our kinetic data showing that all variant (single-substitution) enzymes possessed a significantly reduced catalytic activity for both NCF and ampicillin. In contrast, the R220A-A244R double-mutant enzyme exhibited partial restoration of catalytic activity. All variant enzymes demonstrated a significant increase in both K_i and IC_{50}s for all tested inhibitors, including the carbapenems (imipenem, meropenem, ertapenem, and doripenem). Again, the R220A-A244R enzyme partly restored inhibitor susceptibility (Tables 4 and 5).

Examination of the crystal structure of the R220A mutant; role of a positive charge in BlaC. A crystal of the variant R220A enzyme was generated and analyzed to determine if loss of activity in the R220 variant was caused by a change in the active site structure or by the lack of positive charge provided by the arginine residue. The crystal structure of the R220A variant BlaC enzyme was obtained at 2.1 Å. The crystal belonged to space group $P2_12_12_1$. Refinement statistics are summarized in Table 6.

Comparison of the R220A structure with the wild-type enzyme revealed that the overall structure of the active site is preserved, including the K234-T235-G236 motif (Fig. 2A and B). The structure of R220A also reveals that the T237 side chain is rotated away from the substrate binding cavity and productive interaction is lost (Fig. 2C). Together with the kinetic data, these results show that the positive charge provided by the guanidinium side chain of R220 plays a direct functional role in catalysis.

Effect of inhibitor-resistant mutations on β-lactam susceptibility of *M. tuberculosis*. To assess the impact of substitutions that confer inhibitor resistance on susceptibility of *M. tuberculosis* to β-lactam–β-lactamase inhibitor combinations, the *blaC* mutant alleles were used to complement the *M. tuberculosis* H37RvΔ*blaC1* mutant (38). The *blaC* genes were cloned into the integrative vector pMV361; thus, their expression in mycobacteria is coupled to the heat shock promoter *hsp*60 (37). Expression of BlaC proteins in H37RvΔ*blaC1* was assessed by immunoblotting using the anti-BlaC antibody. Specific recognition of BlaC by the antibody was confirmed, with a detection limit of 8 ng, as assessed by serial dilutions (Fig. 3A). Expression of BlaC proteins was detected in all variant strains by immunoblotting of protein preparations using equal amounts of total protein. Some slight differences in density of the bands were observed (Fig. 3B and C). These apparent differences were compared to wild-type BlaC expression levels using densitometry (http://rsbweb.nih.gov/ij/). Relative expression levels ranged from 0.5 (H37RvΔ*blaC1/blaC*) to 2.7 (H37RvΔ*blaC1*/T237S), with the majority falling between 0.7 and 2.3.

Since clavulanic acid was shown to inactivate BlaC, we focused our analysis on this inhibitor in combination with ampicillin: growth was assessed in the presence of ampicillin (10 μg/ml) alone or ampicillin (10 μg/ml) plus clavulanic acid (5 or 10 μg/ml). These concentrations are clinically relevant (as established by the CLSI in 2008; MICs for susceptible *Enterobacteriaceae* are ≤8 μg/ml for ampicillin and ≤8/4 μg/ml for amoxicillin/clavulanate [52]).

As expected, the wild-type *M. tuberculosis* H37Rv was resistant

TABLE 4 Inhibitor kinetics of variant enzymes compared to the wild type for mechanism-based inhibitors

Mutation(s)	Clavulanate		Sulbactam		Tazobactam	
	K_i (μM)	IC_{50} (μM)	K_i (μM)	IC_{50} (μM)	K_i (μM)	IC_{50} (μM)
None (wild type)	32 ± 1	1.7 ± 0.2	14 ± 1	1.6 ± 0.2	49 ± 3	2.5 ± 0.2
R220A	>100	>100	>100	>100	>100	>100
R220S	>100	>100	>100	>100	>100	>100
R220A, A244R	>100	33 ± 3	>100	23 ± 2	>100	37 ± 4
S130G	>100	>100	>100	108 ± 10	>100	>100
T237A	>100	17 ± 2	>100	16.4 ± 0.2	>100	7.9 ± 0.1
T237S	94 ± 14	6.7 ± 1.2	22 ± 1	0.9 ± 0.2	58 ± 10	1.8 ± 0.2

TABLE 5 Inhibitor kinetics of variant enzymes compared to the wild type for carbapenems

Mutation(s)	Imipenem		Meropenem		Ertapenem		Doripenem	
	K_i (μM)	IC_{50} (μM)	K_i (μM)	IC_{50} (μM)	K_i (μM)	IC_{50} (μM)	K_i (μM)	IC_{50} (μM)
None (wild type)	5 ± 0.4	0.8 ± 0.1	9.0 ± 0.7	0.5 ± 0.05	12.4 ± 1.3	1 ± 0.1	5.6 ± 0.5	0.24 ± 0.02
R220A	>100	90 ± 2.1	>100	>100	>100	>100	>100	70 ± 9
R220S	>100	55 ± 2	>100	>100	>100	>100	>100	96 ± 8
R220A, A244R	>100	23 ± 1	>100	10 ± 1	>100	10 ± 1	>100	6 ± 0.3
S130G	>100	>100	>100	>100	>100	>100	>100	97 ± 9
T237A	>100	62 ± 7	>100	60 ± 5	>100	57 ± 5	>100	38 ± 3
T237S	11.8 ± 1.2	0.8 ± 0.05	13 ± 4	0.53 ± 0.03	25 ± 3	0.58 ± 0.05	10.6 ± 1	0.29 ± 003

to ampicillin but susceptible to ampicillin-clavulanate. In contrast, the Δ*blaC1* deletion mutant was susceptible to both (Fig. 4A and B). Transformation of the plasmid expressing wild-type BlaC (Δ*blaC1*/*blaC*) restored the wild-type phenotype, suggesting that the ampicillin resistance is dependent solely upon BlaC expression. Most importantly, the "inhibitor-resistant" substitutions in BlaC did not result in clavulanic acid resistance. The strain possessing the T237S mutant showed minimal growth in the presence of 5 μg/ml clavulanate, but its growth was inhibited at the higher concentration. This was in contrast to the *in vitro* kinetic analysis that showed impaired catalytic activity and enzymatic resistance against clavulanate.

TABLE 6 Summary of data collection and refinement statistics for the BlaC-R236A mutant apo crystal structure[a]

Statistic or parameter[b]	Value[c]
Wavelength (Å)	1.0
Temperature (K)	100
Resolution range (Å)	50.0–2.1
Reflection	15,203 (4,651)
Completeness (%)	100 (99.68)
$I/\sigma(I)$	40.0 (6.0)
Redundancy	8 (7.3)
Space group	$P2_12_12_1$
Unit cell (Å)	
a	49.41
b	67.43
c	74.63
α = β = γ	90.0°
Molecules per a.u.	1
Refinement statistics	
R_{work} (%)	13.39
R_{free} (%)	17.71
No. of atoms	2,296
Protein (chain A)	1,993
Phosphate	25
Water	278
RMSD	
Bond length (Å)	0.007
Bond angles (°)	1.098
Overall (chain A)	13.88
Protein main chain (chain A)	12.64
Protein side chain (chain A)	15.31
Phosphate	38.29
Water	31.76

[a] The X-ray source was the NSLS beamline X29.
[b] a.u., asymmetric unit; RMSD, root mean square deviation.
[c] Values for the highest-resolution shell are in parentheses.

Assessment of β-lactamase activity after prolonged incubation with clavulanate. The drug susceptibility testing raises the possibility that the prolonged exposure of *M. tuberculosis* to clavulanate due to its extremely slow growth may provide sufficient inhibition in the variant BlaC enzymes despite the *in vitro* kinetics that indicated otherwise. To further test this hypothesis, we incubated wild-type BlaC and variant enzymes at a similar clavulanate concentration (5 μg/ml) for 24 h to obtain serial measurements of enzyme activity. Similar to the wild-type enzyme, the T237A and T237S proteins were completely inactivated within minutes and the R220A-A244R enzyme within 1 h. The remaining mutants were initially unaffected; however, after several hours of incubation, a significant reduction of activity was observed (Fig. 5A and B).

DISCUSSION

The primary goal of our study was to determine if substitutions that are expected to confer resistance to clavulanic acid have a significant effect on *M. tuberculosis* susceptibility to ampicillin-clavulanate. To test this, we constructed a set of variant β-lactamases with substitutions at the R220, S130, and T237 sites. We next examined the crystal structure of the BlaC(R220A) mutant protein to gain further insights. Finally, we assessed the impact of these mutations on β-lactam susceptibility of *M. tuberculosis*. Our analysis provided critical insights regarding the use of this combination in clinical practice.

Role of R220 as a substitute for R244 in BlaC of *M. tuberculosis*; insights from biochemical and structural analyses. Examination of common class A β-lactamases (TEM-1 and SHV-1) shows that the positive charge typically located at R244 plays an important role in substrate binding as part of the carboxylate-binding region, as well as in activation of mechanism-based inhibitors (17–21). In TEM-1, positions R244 and A220 are functionally interchangeable with respect to catalytic efficiency and inhibitor susceptibility (21). In BlaC, position 244 is occupied by an alanine, whereas R220 provides the alternate positive charge corresponding to position R244 in other class A enzymes (35). Similar to R244 in TEM and SHV, the positive guanidinium group of R220 forms a hydrogen bond with the carbonyl oxygen of the G236 peptide backbone and the OH group of T237, both residues of the KTG motif (12, 35, 53, 54) (Fig. 1A and B).

Our kinetic data clearly show that loss of R220 in BlaC renders the enzyme catalytically impaired, more so with the alanine than with the serine substitution. We were unable to determine if this altered activity is due to an elevation of K_m or a reduction in k_{cat}. In

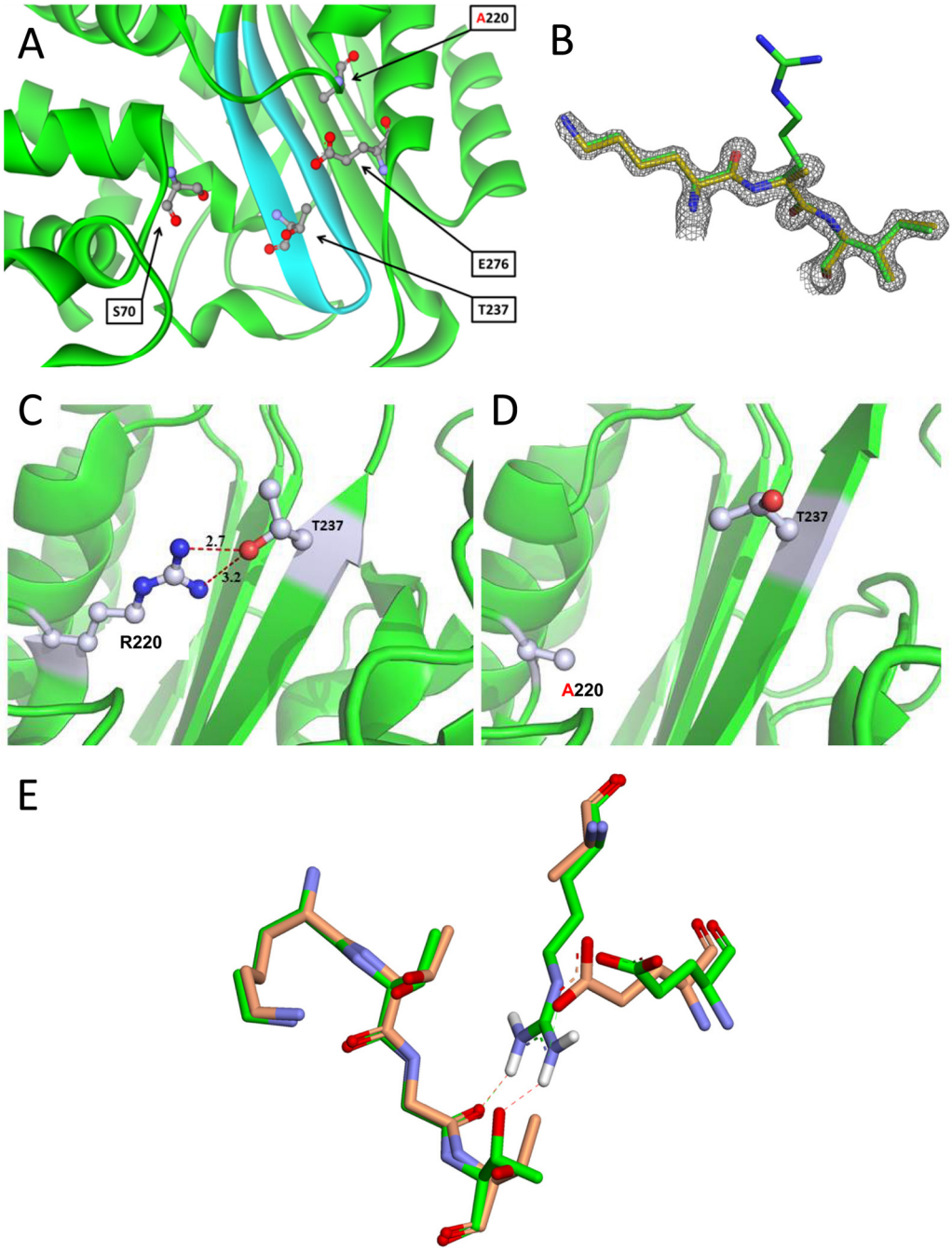

FIG 2 Crystal structure of the R220A variant enzyme. (A) Overall crystal structure. (B) Electron density map for the R220A mutant crystal structure. (C and D) Comparison of the wild type (C) and R220A variant enzyme (D). Note the different orientations of T237 residues. (E) Overlay of KTG motif in the R220A (orange) and E276 (green) enzymes.

parallel with the catalytic impairment, we observed elevated K_i and IC_{50}s for all mechanism-based inhibitors (clavulanic acid, sulbactam, and tazobactam). Interestingly, reintroduction of the positive charge in the 244 region partly restored both catalytic efficiency and inhibitor susceptibility (21).

Comparing our BlaC R220A crystal structure with the wild-type enzyme (PDB entry 2GDN) (35) revealed an overall preservation of the active site with only a minor rotation of the hydroxyl group of T237. As a result, we hypothesize that that R220 serves as a stabilizer of the KTG motif: R220 builds a hydrogen bridge with T237, which allows a productive interaction between the hydroxyl group of T237 and the carboxyl-group of the substrate (Fig. 2C). In Ambler class A enzymes, position 276 is usually occupied by asparagine, whereas in BlaC this is occupied by glutamate. Interestingly, TEM variant enzymes with an N276D substitution are inhibitor resistant. It is thought that the negative charge of the aspartate neutralizes the positive charge of the R244 guanidinium group (55). In BlaC, E276 is in close proximity to R220 (2.6 Å),

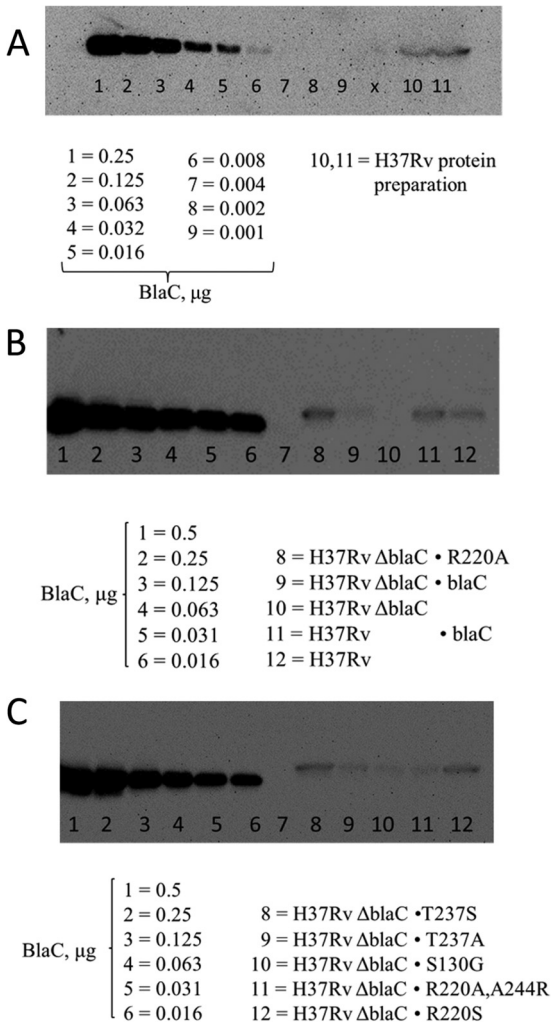

FIG 3 Protein expression of BlaC in *M. tuberculosis*. Immunoblotting was carried out using a rabbit raised polyclonal antibody against BlaC. (A) Expression of BlaC in H37Rv. (B and C) Expression of variant BlaC in H37RvΔ*blaC* mutants.

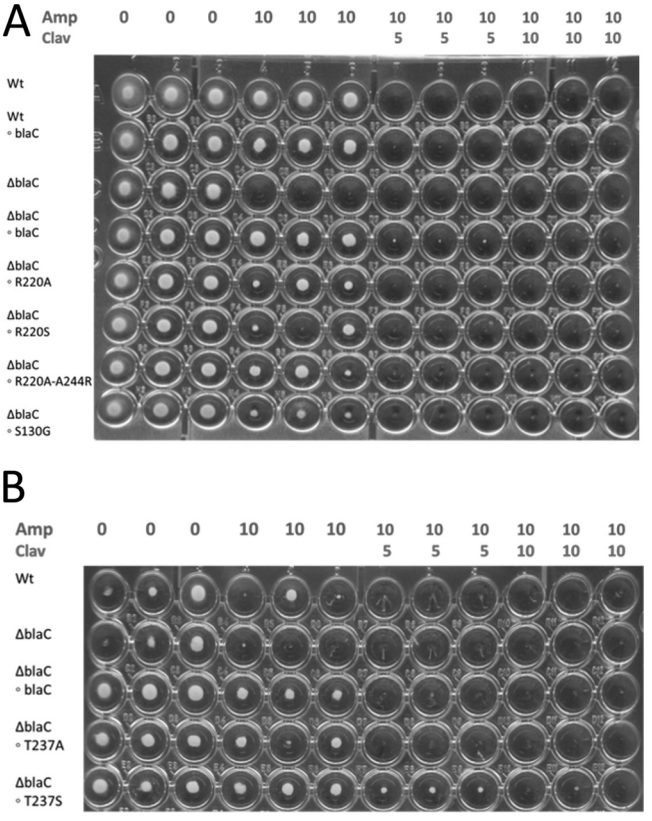

FIG 4 *M. tuberculosis* H37Rv susceptibility assay with ampicillin with and without clavulanate. (A and B) Susceptibility assay. Visually detectable growth after 14 days incubation indicates resistance. Concentrations are in µg/ml.

already weakening the positive charge of guanidinium. In the R220A variant enzyme, this glutamate side chain is shifted toward the KTG motif, where it may provide an unopposed negative charge, leading to profound impairment of substrate and inhibitor binding (Fig. 2D).

Does BlaC require a strategically positioned water molecule to be inactivated by clavulanate? The secondary ring opening of clavulanate requires a strategically positioned water molecule which donates a proton for saturation of the double bond at position C2 (32). In TEM β-lactamases, R244 coordinates this water molecule (32). In SHV, a water molecule is not readily seen in the crystal structure of the apo-enzyme (PDB entry 1SHV) (56). On the basis of mutagenesis studies, Thomson et al. suggested that the coordinating water molecule is recruited from the solvent during substrate interaction (34). A review of the available BlaC-ligand structures reveals differences with regard to the role of water molecules. In the structure of the apo-enzyme, no water molecule coordinated by R220 is seen (PDB entry 2GDN) (35). Similarly, the interaction of the C4 carboxylate group of cefamandole with S130, T235, T237, and possibly R220 (shortest distance = 3.6 Å) takes place without evidence of a water molecule in both K73A (PDB entry 3NY4) and E166A (PDB entry 3N8S) enzyme structures (15). In contrast, the C3 group of meropenem, in an orientation similar to that of the carboxylate group of clavulanate, binds to T235 and a coordinated water molecule, which forms a hydrogen bond to the carbonyl oxygen of T216 and the guanidinium group of R220 (Fig. 6A and B) (PDB entry 3DWZ) (12). Unlike R244 in SHV-1, R220 in BlaC does not interact directly with the C3 carboxylate of meropenem. A careful examination of our R220A structure revealed that a water molecule is present in a location similar to that of the BlaC-meropenem structure, which is in contrast to the apo-enzyme structure.

Based on the crystal structure of BlaC with meropenem, we have created a model of the Michaelis complex of clavulanate and BlaC with a water molecule in the active site (Fig. 6C). We propose that the guanidinium group on R220 serves to polarize the water molecule in order to allow donation of the proton, which allows secondary ring opening of clavulanate (Fig. 6A and B; shortest distance to guanidinium group = 3.3 Å).

Role of S130 in BlaC. S130 is a conserved amino acid residue among class A enzymes and plays an important role in substrate binding and proton donation during β-lactam ring opening (57, 58). Furthermore, S130 is an important residue for mechanism-based inhibitors: the serine hydroxyl group can form a second covalent bond with reactive intermediates of the inhibitor, leading to cross-linking of the inhibitor within the active site (59). The

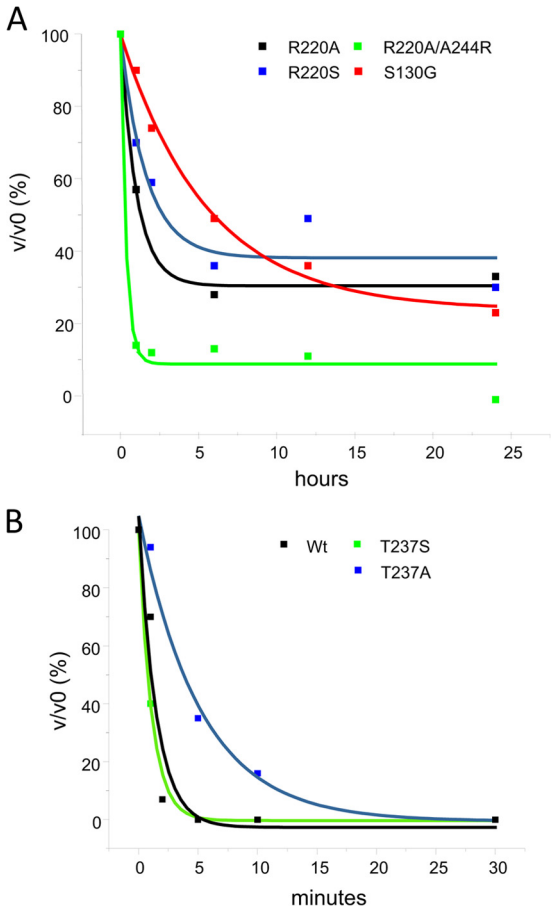

FIG 5 Time-dependent enzyme inactivation by clavulanate (5 μg/ml). The curves represent best fits for first-order decay. Note the different time scales of the plots. (A) Slow deactivation within hours. Note the small residual activity of the R220A, R220S, and S130G enzymes after 24 h (around 30%). (B) Rapid deactivation within minutes. No recovery of activity was detected at 24 h (data not shown).

latter step seems to be important for permanent inactivation of certain β-lactamases. Indeed, several inhibitor-resistant class A variant enzymes which bear a serine-to-glycine mutation have been described (60–62).

In both TEM and SHV enzymes, the missing serine hydroxyl group is partly compensated for by a repositioned water molecule (62, 63), leading to altered catalytic activity. Furthermore, the S130G mutant enzymes exhibit high K_i values and lower partition ratios (k_{cat}/k_{inact}), which can result in an inhibitor-resistant phenotype (62). In accordance with other class A enzymes, the S130G variant of BlaC clearly demonstrates resistance to mechanism-based inhibitors, as well as carbapenems, which parallels significant loss of catalytic activity. This will be pursued further.

Role of T237 in BlaC. Position 237 in the majority of β-lactamases is occupied by alanine or serine, and its functional importance is seen in the backbone nitrogen that forms, in conjunction with serine 70, the oxyanion hole. This oxyanion hole positions the carbonyl oxygen of the β-lactam during hydrolysis (64). While BlaC is effectively inhibited by carbapenems, this β-lactamase shares the threonine residue at position 237 with class A carbapenemases, most notably KPC-2 (65). T237 acts as an important residue in binding of the carboxylate group of β-lactams, as has been shown in the crystal structures of BlaC with carbapenems and cefamandole (14, 15). Notably, T237 also interacts with the R220 residue as detailed above. Based on these observations and recent data from studies with KPC-2 mutants, we suspect that mutations at this position may alter inhibitor susceptibility in BlaC (66).

In contrast to all other variations, the T237S mutation led to only minor impairment of catalytic function due to an increased K_m value (130 ± 4 μM versus 56 ± 4 μM, resulting in a >50% reduction of NCF hydrolysis). In parallel, modest increases in K_i were observed for clavulanate (3×) and sulbactam (2×), but no increase was observed for tazobactam. Similarly, IC_{50}s for clavulanate and sulbactam nearly doubled, while IC_{50}s for tazobactam were essentially unchanged. Overall, based on IC_{50}s, all inhibitors retained their activity against the T237S variant enzyme.

The T237A variant of BlaC resulted in a 50-fold reduction of NCF hydrolytic activity, driven by both an increase of the K_m value and a decrease of k_{cat}. Similarly, the K_i values for all tested inhibitors as well as carbapenems were >100 μM, and IC_{50}s for clavulanate, sulbactam, and tazobactam were increased 10- to 35-fold.

In summary, while the T237S mutation had a modest impact on increasing inhibitor resistance, the T237A variant enzyme resulted in a remarkable increase in resistance to inhibitors and to carbapenems, but at the cost of a significant reduction in catalytic activity. With the exception of T237S, all variant enzymes showed impaired susceptibility to mechanism-based inhibitors and carbapenems.

Correlation between enzyme kinetics and *M. tuberculosis* drug susceptibility: growth, cell wall turnover, and protein turnover rates. To our knowledge, this is the first study that assessed the impact of BlaC mutations on *in vivo* susceptibility of *M. tuberculosis*. Surprisingly, the introduction of substitutions into *M. tuberculosis* did not lead to ampicillin-clavulanate resistance in broth cultures. We were able to restore the wild-type resistance profile by complementing the BlaC deletion mutant with a plasmid bearing the native *blaC* sequence, which supports our chosen model. Furthermore, BlaC expression was detected for all mutant strains by immunoblot analysis, with minor differences in expression level between the engineered variants. Remarkably, all mutant strains exhibited low-level ampicillin resistance, indicating sufficient expression of BlaC, and even mutants that generated enzymes with high-level *in vitro* resistance to clavulanate continued to be susceptible to clavulanate in broth culture within the tested range. This is in stark contrast to work similarly done in Gram-negative bacteria (see reference 64 for a review), which reveals generally good correlations between kinetic data and susceptibility testing, after accounting for differences in expression level.

Our data nicely demonstrate that there is a startling difference between kinetic data and mycobacterial susceptibility testing. Growth kinetics and cell wall turnover in mycobacteria are remarkably slow compared to those in Gram-negative bacteria. We postulate that kinetic data derived from observations over minutes may not reflect the true impact of β-lactam–inhibitor combinations on mycobacterial growth. To support this, we incubated our mutant enzymes with clavulanate for a prolonged period of time at a concentration of 5 μg/ml, similar to the concentration used in the susceptibility testing of *M. tuberculosis*. Our results were notable. First, measurement of β-lactamase activity after a period of hours revealed that even highly resistant enzymes even-

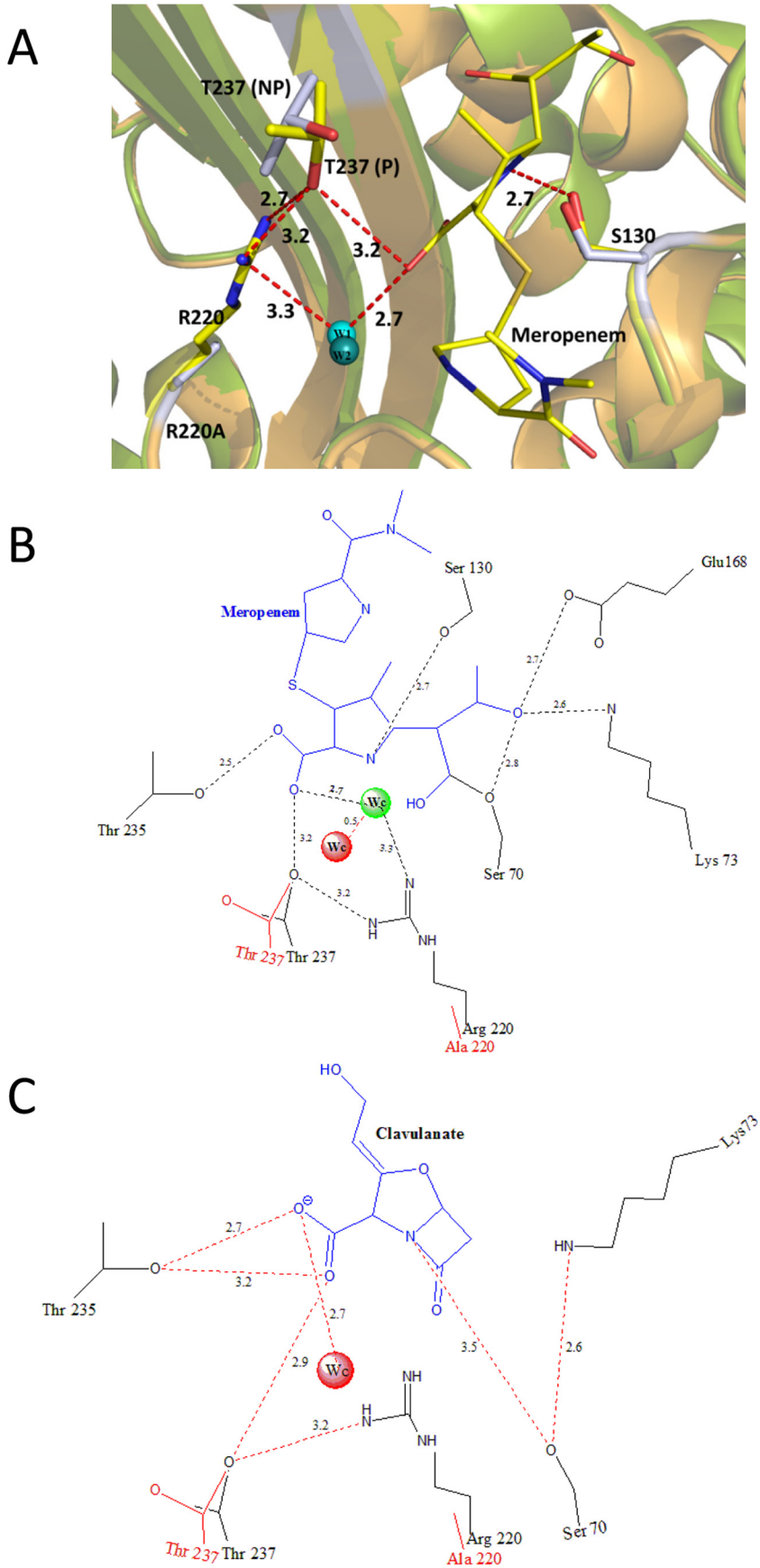

FIG 6 Model of the role of R220 in substrate binding. (A) Comparison between the wild-type BlaC-meropenem-bound structure (green) and the R220A variant enzyme (orange). W1, water from 3DWZ (wild-type BlaC-meropenem-bound) crystal structure; W2, water from the BlaC R220A mutant structure. (B) Impact of the R220A substitution on the T237 residue and binding of meropenem. (C) Model of clavulanate. The BlaC Michaelis complex shows the impact of R220A.

tually were inactivated by clavulanate. Second, as expected, this process follows a first-order-decay kinetic behavior (Fig. 5) with remarkable differences in enzyme half-life: the wild type and the T237A and T237S mutants were completely inactivated within a few minutes (Fig. 5A), the R220A-A244R enzyme was inactivated within 1 h, and the R220A, R220S, and S130G enzymes were inactivated only after a period of several hours (Fig. 5B). The latter group did have about 30% residual activity at 24 h. Lastly, the rate of inactivation corresponded well to the determined IC_{50}s for clavulanate of the mutant enzymes: the higher the value, the longer the time to inactivation.

The interaction of mechanism-based inhibitors with enzymes may be paradoxical; i.e., inhibitors with low K_is may initially inactivate the enzyme but eventually undergo hydrolysis with subsequent slow recovery. This was not the case for the tested BlaC variant enzymes; a gain in function was not observed at 24 h, indicating prolonged inactivation of the enzymes, which is in concordance with the observed resistance patterns *in vivo*. In contrast, for BlaC inhibition with sulbactam and tazobactam, but not with clavulanate, substantial recovery of enzyme activity has been observed within 1 h (67). On the other hand, it has been shown for S130G mutations in SHV that impaired inhibitor affinity may result in relative inhibitor resistance, which still can lead to progressive loss of enzyme activity with time, due to the permanent nature of the inactivation (63). Given the very high K_i values for all tested inhibitors, we propose that a model that implies decreased affinity is most consistent with our observations.

In conclusion, the *in vivo* inhibitor resistance phenotype is a function of time-dependent inactivation of the β-lactamase and growth rate of the bacteria of interest. Given that the generation time of *M. tuberculosis* is close to a day, slow irreversible inhibition can overcome relative inhibitor resistance.

Implications for clinical treatment. Our results favor the notion of BlaC being an important therapeutic target, and we are cautiously optimistic that resistance to β-lactam combinations with clavulanate will not arise on the basis of structural alteration of the enzyme. This is favored by the long generation time and the irreversible nature of inhibition. Given the propensity of *M. tuberculosis* for generating resistance to all classes of agents in clinical use, we expect that resistance to β-lactam combinations will follow the same path, and more studies, including epidemiological surveys in areas with high β-lactam antibiotic use, are needed in order to determine potential resistance mechanisms. This may occur at different levels, including membrane transport/permeability, alterations in penicillin-binding proteins, and regulation of BlaC expression, but is less likely to occur on the basis of yet-unrecognized mutations in the BlaC enzyme (68).

ACKNOWLEDGMENTS

We thank M. Pavelka for the generous gift of the BlaC-deficient *M. tuberculosis* strain PM638.

Research reported in this publication was supported by the National Institute of Allergy and Infectious Diseases of the National Institutes of Health under award numbers R01AI072219, R01AI063517, and R01AI100560 to R.A.B. and RO1AI060899 to J.S.B. This study was supported in part by funds and/or facilities provided by the Cleveland Department of Veterans Affairs, the Veterans Affairs Merit Review Program, and the Geriatric Research Education and Clinical Center VISN 10 to R.A.B. This study was supported by the Charles H. Revson foundation (L.T.).

The content is solely the responsibility of the authors and does not necessarily represent the official views of the National Institutes of Health or the Veterans Administration.

REFERENCES

1. **WHO.** 2011. Global tuberculosis control: WHO report 2011. WHO, Geneva, Switzerland.
2. **WHO.** 2010. Multidrug and extensively drug-resistant TB (M/XDR-TB): 2010 global report on surveillance and response. WHO, Geneva, Switzerland.
3. **Gandhi NR, Moll A, Sturm AW, Pawinski R, Govender T, Lalloo U, Zeller K, Andrews J, Friedland G.** 2006. Extensively drug-resistant tuberculosis as a cause of death in patients co-infected with tuberculosis and HIV in a rural area of South Africa. Lancet **368:**1575–1580.
4. **Chambers HF, Moreau D, Yajko D, Miick C, Wagner C, Hackbarth C, Kocagoz S, Rosenberg E, Hadley WK, Nikaido H.** 1995. Can penicillins and other beta-lactam antibiotics be used to treat tuberculosis? Antimicrob. Agents Chemother. **39:**2620–2624.
5. **Hackbarth CJ, Unsal I, Chambers HF.** 1997. Cloning and sequence analysis of a class A beta-lactamase from *Mycobacterium tuberculosis* H37Ra. Antimicrob. Agents Chemother. **41:**1182–1185.
6. **Voladri RK, Lakey DL, Hennigan SH, Menzies BE, Edwards KM, Kernodle DS.** 1998. Recombinant expression and characterization of the major beta-lactamase of *Mycobacterium tuberculosis*. Antimicrob. Agents Chemother. **42:**1375–1381.
7. **Ambler RP, Coulson AF, Frere JM, Ghuysen JM, Joris B, Forsman M, Levesque RC, Tiraby G, Waley SG.** 1991. A standard numbering scheme for the class A beta-lactamases. Biochem. J. **276:**269–270.
8. **Cynamon MH, Palmer GS.** 1983. In vitro activity of amoxicillin in combination with clavulanic acid against *Mycobacterium tuberculosis*. Antimicrob. Agents Chemother. **24:**429–431.
9. **Casal M, Rodriguez F, Benavente M, Luna M.** 1986. In vitro susceptibility of *Mycobacterium tuberculosis*, *Mycobacterium fortuitum* and *Mycobacterium chelonei* to augmentin. Eur. J. Clin. Microbiol. **5:**453–454.
10. **Tremblay LW, Hugonnet JE, Blanchard JS.** 2008. Structure of the covalent adduct formed between *Mycobacterium tuberculosis* beta-lactamase and clavulanate. Biochemistry **47:**5312–5316.
11. **Chambers HF, Kocagoz T, Sipit T, Turner J, Hopewell PC.** 1998. Activity of amoxicillin/clavulanate in patients with tuberculosis. Clin. Infect. Dis. **26:**874–877.
12. **Hugonnet JE, Tremblay LW, Boshoff HI, Barry CE, III, Blanchard JS.** 2009. Meropenem-clavulanate is effective against extensively drug-resistant *Mycobacterium tuberculosis*. Science **323:**1215–1218.
13. **Dauby N, Muylle I, Mouchet F, Sergysels R, Payen MC.** 2011. Meropenem/clavulanate and linezolid treatment for extensively drug-resistant tuberculosis. Pediatr. Infect. Dis. J. **30:**812–813.
14. **Tremblay LW, Fan F, Blanchard JS.** 2010. Biochemical and structural characterization of *Mycobacterium tuberculosis* beta-lactamase with the carbapenems ertapenem and doripenem. Biochemistry **49:**3766–3773.
15. **Tremblay LW, Xu H, Blanchard JS.** 2010. Structures of the Michaelis complex (1.2 A) and the covalent acyl intermediate (2.0 A) of cefamandole bound in the active sites of the *Mycobacterium tuberculosis* beta-lactamase K73A and E166A mutants. Biochemistry **49:**9685–9687.
16. **Strynadka NC, Adachi H, Jensen SE, Johns K, Sielecki A, Betzel C, Sutoh K, James MN.** 1992. Molecular structure of the acyl-enzyme intermediate in beta-lactam hydrolysis at 1.7 A resolution. Nature **359:**700–705.
17. **Zafaralla G, Manavathu EK, Lerner SA, Mobashery S.** 1992. Elucidation of the role of arginine-244 in the turnover processes of class A beta-lactamases. Biochemistry **31:**3847–3852.
18. **Jacob-Dubuisson F, Lamotte-Brasseur J, Dideberg O, Joris B, Frere JM.** 1991. Arginine 220 is a critical residue for the catalytic mechanism of the *Streptomyces albus* G beta-lactamase. Protein Eng. **4:**811–819.
19. **Ishii Y, Ohno A, Taguchi H, Imajo S, Ishiguro M, Matsuzawa H.** 1995. Cloning and sequence of the gene encoding a cefotaxime-hydrolyzing class A beta-lactamase isolated from *Escherichia coli*. Antimicrob. Agents Chemother. **39:**2269–2275.
20. **Matagne A, Lamotte-Brasseur J, Frere JM.** 1998. Catalytic properties of class A beta-lactamases: efficiency and diversity. Biochem. J. **330:**581–598.
21. **Marciano DC, Brown NG, Palzkill T.** 2009. Analysis of the plasticity of

location of the Arg244 positive charge within the active site of the TEM-1 beta-lactamase. Protein Sci. **18:**2080–2089.
22. **Frase H, Shi Q, Testero SA, Mobashery S, Vakulenko SB.** 2009. Mechanistic basis for the emergence of catalytic competence against carbapenem antibiotics by the GES family of beta-lactamases. J. Biol. Chem. **284:**29509–29513.
23. **Ke W, Bethel CR, Thomson JM, Bonomo RA, van den Akker F.** 2007. Crystal structure of KPC-2: insights into carbapenemase activity in class A beta-lactamases. Biochemistry **46:**5732–5740.
24. **Blazquez J, Negri MC, Morosini MI, Gomez-Gomez JM, Baquero F.** 1998. A237T as a modulating mutation in naturally occurring extended-spectrum TEM-type beta-lactamases. Antimicrob. Agents Chemother. **42:**1042–1044.
25. **Bouthors AT, Delettre J, Mugnier P, Jarlier V, Sougakoff W.** 1999. Site-directed mutagenesis of residues 164, 170, 171, 179, 220, 237 and 242 in PER-1 beta-lactamase hydrolysing expanded-spectrum cephalosporins. Protein Eng. **12:**313–318.
26. **Gazouli M, Tzelepi E, Sidorenko SV, Tzouvelekis LS.** 1998. Sequence of the gene encoding a plasmid-mediated cefotaxime-hydrolyzing class A beta-lactamase (CTX-M-4): involvement of serine 237 in cephalosporin hydrolysis. Antimicrob. Agents Chemother. **42:**1259–1262.
27. **Giakkoupi P, Hujer AM, Miriagou V, Tzelepi E, Bonomo RA, Tzouvelekis LS.** 2001. Substitution of Thr for Ala-237 in TEM-17, TEM-12 and TEM-26: alterations in beta-lactam resistance conferred on *Escherichia coli*. FEMS Microbiol. Lett. **201:**37–40.
28. **Majiduddin FK, Palzkill T.** 2005. Amino acid residues that contribute to substrate specificity of class A beta-lactamase SME-1. Antimicrob. Agents Chemother. **49:**3421–3427.
29. **Sougakoff W, Naas T, Nordmann P, Collatz E, Jarlier V.** 1999. Role of ser-237 in the substrate specificity of the carbapenem-hydrolyzing class A beta-lactamase Sme-1. Biochim. Biophys. Acta **1433:**153–158.
30. **Tamaki M, Nukaga M, Sawai T.** 1994. Replacement of serine 237 in class A beta-lactamase of *Proteus vulgaris* modifies its unique substrate specificity. Biochemistry **33:**10200–10206.
31. **Brenner DG, Knowles JR.** 1981. Penicillanic acid sulfone: an unexpected isotope effect in the interaction of 6 alpha- and 6 beta-monodeuterio and of 6,6-dideuterio derivatives with RTEM beta-lactamase from *Escherichia coli*. Biochemistry **20:**3680–3687.
32. **Imtiaz U, Billings E, Knox JR, Manavathu EK, Lerner SA, Mobashery S.** 1993. Inactivation of class A β-lactamases by clavulanic acid: the role of arginine-244 in a proposed nonconcerted sequence of events. J. Am. Chem. Soc. **115:**4435–4442.
33. **Kalp M, Totir MA, Buynak JD, Carey PR.** 2009. Different intermediate populations formed by tazobactam, sulbactam, and clavulanate reacting with SHV-1 beta-lactamases: Raman crystallographic evidence. J. Am. Chem. Soc. **131:**2338–2347.
34. **Thomson JM, Distler AM, Prati F, Bonomo RA.** 2006. Probing active site chemistry in SHV beta-lactamase variants at Ambler position 244. Understanding unique properties of inhibitor resistance. J. Biol. Chem. **281:**26734–26744.
35. **Wang F, Cassidy C, Sacchettini JC.** 2006. Crystal structure and activity studies of the *Mycobacterium tuberculosis* beta-lactamase reveal its critical role in resistance to beta-lactam antibiotics. Antimicrob. Agents Chemother. **50:**2762–2771.
36. **Hujer AM, Hujer KM, Helfand MS, Anderson VE, Bonomo RA.** 2002. Amino acid substitutions at Ambler position Gly238 in the SHV-1 beta-lactamase: exploring sequence requirements for resistance to penicillins and cephalosporins. Antimicrob. Agents Chemother. **46:**3971–3977.
37. **Stover CK, de la Cruz VF, Fuerst TR, Burlein JE, Benson LA, Bennett LT, Bansal GP, Young JF, Lee MH, Hatfull GF, et al.** 1991. New use of BCG for recombinant vaccines. Nature **351:**456–460.
38. **Flores AR, Parsons LM, Pavelka MS, Jr.** 2005. Genetic analysis of the beta-lactamases of *Mycobacterium tuberculosis* and *Mycobacterium smegmatis* and susceptibility to beta-lactam antibiotics. Microbiology **151:**521–532.
39. **Braunstein M, Bardarov SS, Jacobs WR, Jr.** 2002. Genetic methods for deciphering virulence determinants of *Mycobacterium tuberculosis*. Methods Enzymol. **358:**67–99.
40. **Wallace RJ, Jr, Nash DR, Steele LC, Steingrube V.** 1986. Susceptibility testing of slowly growing mycobacteria by a microdilution MIC method with 7H9 broth. J. Clin. Microbiol. **24:**976–981.
41. **Otwinowski Z, Minor W.** 1997. Processing of X-ray diffraction data collected in oscillation mode. Methods Enzymol. **276:**307–326.
42. **Potterton E, Briggs P, Turkenburg M, Dodson E.** 2003. A graphical user interface to the CCP4 program suite. Acta Crystallogr. D Biol. Crystallogr. **59:**1131–1137.
43. **Murshudov GN, Vagin AA, Dodson EJ.** 1997. Refinement of macromolecular structures by the maximum-likelihood method. Acta Crystallogr. D Biol. Crystallogr. **53:**240–255.
44. **Pannu NS, Murshudov GN, Dodson EJ, Read RJ.** 1998. Incorporation of prior phase information strengthens maximum-likelihood structure refinement. Acta Crystallogr. D Biol. Crystallogr. **54:**1285–1294.
45. **Adams PD, Afonine PV, Bunkoczi G, Chen VB, Davis IW, Echols N, Headd JJ, Hung LW, Kapral GJ, Grosse-Kunstleve RW, McCoy AJ, Moriarty NW, Oeffner R, Read RJ, Richardson DC, Richardson JS, Terwilliger TC, Zwart PH.** 2010. PHENIX: a comprehensive Python-based system for macromolecular structure solution. Acta Crystallogr. D Biol. Crystallogr. **66:**213–221.
46. **Emsley P, Cowtan K.** 2004. Coot: model-building tools for molecular graphics. Acta Crystallogr. D Biol. Crystallogr. **60:**2126–2132.
47. **DeLano WL.** 2002. The PyMOL molecular graphics system. DeLano Scientific, San Carlos, CA.
48. **Laskowski RA.** 2009. PDBsum new things. Nucleic Acids Res. **37:**D355–D359.
49. **Hess B, Kutzner C, van der Spoel D, Lindahl E.** 2008. GROMACS 4: algorithms for highly efficient, load-balanced, and scalable molecular simulation. J. Chem. Theory Comput. **4:**435–447.
50. **Lindahl B, Hess D, Van der Spoel D.** 2001. Gromacs 3.0: a package for molecular simulation and trajectory analysis. J. Mol. Model. **7:**306–317.
51. **Vaught A.** 1996. Graphing with Gnuplot and Xmgr. Linux J. http://www.linuxjournal.com/article/1218.
52. **CLSI.** 2008. Performance standards for antimicrobial susceptibility testing. Eighteenth informational supplement. CLSI document M100-S18. Clinical Laboratory Standards Institute, Wayne, PA.
53. **Nukaga M, Bethel CR, Thomson JM, Hujer AM, Distler A, Anderson VE, Knox JR, Bonomo RA.** 2008. Inhibition of class A beta-lactamases by carbapenems: crystallographic observation of two conformations of meropenem in SHV-1. J. Am. Chem. Soc. **130:**12656–12662.
54. **Jelsch C, Mourey L, Masson JM, Samama JP.** 1993. Crystal structure of *Escherichia coli* TEM1 beta-lactamase at 1.8 A resolution. Proteins **16:**364–383.
55. **Swaren P, Maveyraud L, Guillet V, Masson JM, Mourey L, Samama JP.** 1995. Electrostatic analysis of TEM1 beta-lactamase: effect of substrate binding, steep potential gradients and consequences of site-directed mutations. Structure **3:**603–613.
56. **Kuzin AP, Nukaga M, Nukaga Y, Hujer AM, Bonomo RA, Knox JR.** 1999. Structure of the SHV-1 beta-lactamase. Biochemistry **38:**5720–5727.
57. **Lamotte-Brasseur J, Dive G, Dideberg O, Charlier P, Frere JM, Ghuysen JM.** 1991. Mechanism of acyl transfer by the class A serine beta-lactamase of *Streptomyces albus* G. Biochem. J. **279:**213–221.
58. **Atanasov BP, Mustafi D, Makinen MW.** 2000. Protonation of the beta-lactam nitrogen is the trigger event in the catalytic action of class A beta-lactamases. Proc. Natl. Acad. Sci. U. S. A. **97:**3160–3165.
59. **Kuzin AP, Nukaga M, Nukaga Y, Hujer A, Bonomo RA, Knox JR.** 2001. Inhibition of the SHV-1 beta-lactamase by sulfones: crystallographic observation of two reaction intermediates with tazobactam. Biochemistry **40:**1861–1866.
60. **Bermudes H, Jude F, Chaibi EB, Arpin C, Bebear C, Labia R, Quentin C.** 1999. Molecular characterization of TEM-59 (IRT-17), a novel inhibitor-resistant TEM-derived beta-lactamase in a clinical isolate of *Klebsiella oxytoca*. Antimicrob. Agents Chemother. **43:**1657–1661.
61. **Prinarakis EE, Miriagou V, Tzelepi E, Gazouli M, Tzouvelekis LS.** 1997. Emergence of an inhibitor-resistant beta-lactamase (SHV-10) derived from an SHV-5 variant. Antimicrob. Agents Chemother. **41:**838–840.
62. **Thomas VL, Golemi-Kotra D, Kim C, Vakulenko SB, Mobashery S, Shoichet BK.** 2005. Structural consequences of the inhibitor-resistant Ser130Gly substitution in TEM beta-lactamase. Biochemistry **44:**9330–9338.
63. **Helfand MS, Bethel CR, Hujer AM, Hujer KM, Anderson VE, Bonomo RA.** 2003. Understanding resistance to beta-lactams and beta-lactamase inhibitors in the SHV beta-lactamase: lessons from the mutagenesis of SER-130. J. Biol. Chem. **278:**52724–52729.
64. **Drawz SM, Bonomo RA.** 2010. Three decades of beta-lactamase inhibitors. Clin. Microbiol. Rev. **23:**160–201.

65. **Papp-Wallace KM, Taracila M, Hornick JM, Hujer AM, Hujer KM, Distler AM, Endimiani A, Bonomo RA.** 2010. Substrate selectivity and a novel role in inhibitor discrimination by residue 237 in the KPC-2 beta-lactamase. Antimicrob. Agents Chemother. **54:**2867–2877.
66. **Papp-Wallace KM, Taracila MA, Smith KM, Xu Y, Bonomo RA.** 2012. Understanding the molecular determinants of substrate and inhibitor specificities in the carbapenemase KPC-2: exploring the roles of Arg220 and Glu276. Antimicrob. Agents Chemother. **56:**4428–4438.
67. **Hugonnet JE, Blanchard JS.** 2007. Irreversible inhibition of the *Mycobacterium tuberculosis* beta-lactamase by clavulanate. Biochemistry **46:** 11998–12004.
68. **Sala C, Haouz A, Saul FA, Miras I, Rosenkrands I, Alzari PM, Cole ST.** 2009. Genome-wide regulon and crystal structure of BlaI (Rv1846c) from *Mycobacterium tuberculosis*. Mol. Microbiol. **71:**1102–1116.
69. **Trott O, Olson AJ.** 2010. AutoDock Vina: improving the speed and accuracy of docking with a new scoring function, efficient optimization and multithreading. J. Comput. Chem. **31:**455–461.
70. **Li Z, Wan H, Shi Y, Ouyang P.** 2004. Personal experience with four kinds of chemical structure drawing software: review on ChemDraw, ChemWindow, ISIS/Draw, and ChemSketch. J. Chem. Inf. Comput. Sci. **44:** 1886–1890.
71. **Morris GM, Goodsell DS, Halliday RS, Huey R, Hart WE, Belew RK, Olson AJ.** 1998. Automated docking using a Lamarckian genetic algorithm and empirical binding free energy function. J. Comput. Chem. **19:** 1639–1662.
72. **Schüttelkopf AW, van Aalten DMF.** 2004. PRODRG: a tool for high-throughput crystallography of protein-ligand complexes. Acta Crystallogr. D **60:**1355–1363.